

## First-principles investigation of the quantum-well system Na on Cu(111)

Johan M. Carlsson and Bo Hellsing

*Department of Physics, Chalmers University of Technology and Göteborg University, SE-412 96 Gothenburg, Sweden*

(Received 16 July 1999; revised manuscript received 12 January 2000)

The alkali-metal adsorption system Na on Cu(111) has been investigated theoretically in order to clarify the possible presence of quantum-well states observed in photoemission experiments. We analyze the site preference, bonding character, the coverage dependence of the work function, and the electron structure of the system. The study is based on *first-principles* calculations of free-standing Na layers in vacuum, the clean Cu(111) surface, and the Na/Cu(111) adsorption system at two different adsorbate structures:  $(2 \times 2)$  and  $(3/2 \times 3/2)$ . We are able to identify Na-induced bands, which are essentially localized in the local band gap of the Cu(111) surface. The local density of states at the  $\bar{\Gamma}$  point for the lowest of these bands has maxima within the Na adlayer and decays rapidly into the substrate. The dispersion of the Na-induced bands is in good agreement with photoemission data and the  $\bar{\Gamma}$  point energy of the lowest Na-induced band shifts from 0.45 eV above the Fermi level for the  $(2 \times 2)$  structure to 0.06 eV below the Fermi level for the saturated monolayer. We conclude that the Na-induced states have the characteristics of quantum-well states, which supports previous interpretations based on photoemission experiments.

### I. INTRODUCTION

The properties of alkali metals adsorbed on close-packed metal surfaces have been studied for a long time since these systems have been considered as prototype systems of metal on metal adsorption. The investigations have involved the whole coverage range from the low-coverage regime of isolated alkali-metal atom adsorption to the many-layer regime.

An extensive review of experimental and theoretical studies on alkali metals on metal surfaces can be found in the articles by Diehl and McGrath<sup>1</sup> and Stampfl and Scheffler.<sup>2</sup> From an application point of view, the question of how the adsorption of alkali metals changes the properties of the substrate is interesting. In this context many studies concern alkali-metal promoted catalysis on noble metal and semi-metal surfaces.<sup>3,4</sup> Some of the alkali-metal adsorption systems provide the possibility of constructing metallic quantum wells with a quasi-two-dimensional electron gas effectively confined between the substrate and the vacuum barrier.<sup>5,6</sup> The formation of metallic quantum-well states opens up new possibilities in construction of metal-based electronic devices.

In the present study we focused on the model system Na on Cu(111). There is a large amount of experimental data which indicate the existence of quantum-well states within the Na adlayer, but there are no *first-principles* calculations available for this system to confirm the conclusions from experiments. Before giving the details of the calculations, we will review some relevant experimental studies of alkali-metal adsorption on metal surfaces, in particular Na on Cu(111).

Alkali-metal atoms adsorbed on close-packed (111) surfaces of metals have been observed to form hexagonal structures at saturated monolayer coverages following the underlying substrate structure.<sup>1</sup> However, the nearest-neighbor distance in the saturated alkali-metal monolayer is most often larger than in the underlying substrate, because of the large radius of the valence orbital of the alkali-metal atoms.

For instance, potassium has been observed to form a  $(2 \times 2)$  structure on Cu and Ni (111) surfaces.<sup>7</sup> For alkali-metal atoms the adsorption site preference turns out to be size dependent.<sup>1</sup> Alkali-metal atoms with a larger radius of the valence orbital than sodium prefer to sit in an on-top site, while lithium prefers hollow sites at low temperatures and even disrupts the substrate surface at higher temperatures.<sup>8</sup>

The adsorption structure of the Na atoms on the Cu(111) surface has been investigated by low-energy electron-diffraction (LEED) experiments and there is general agreement<sup>1</sup> that the monolayer saturation occurs at the coverage  $\theta = 4/9 \approx 0.44$ , where the coverage is defined as the ratio of Na adatoms to the number of Cu surface atoms. The Na atoms in the saturated monolayer have a hexagonal  $(3/2 \times 3/2)$  structure and the Na atom-atom distance is close to the nearest-neighbor distance in bulk sodium. At coverages below the saturated monolayer, opinions about the adsorption structure differ. Early LEED experiments by Lindgren and Walldén<sup>9</sup> and Dudde *et al.*<sup>10</sup> suggested that the Na atoms form an ordered hexagonal  $(2 \times 2)$  structure already at  $\theta \approx 1/4$  coverage. Later LEED experiments by Tang *et al.*<sup>11</sup> showed a ring pattern in the coverage range  $\theta = 0.1 - 0.35$ , which indicated a less ordered adsorbate liquid behavior described by an effective nearest-neighbor distance. They observed an ordered hexagonal adsorbate structure above  $\theta \approx 0.38$  and confirmed that the monolayer saturation occurs at  $\theta = 4/9$ .

The LEED experiments show a hexagonal adsorbate structure at saturated monolayer coverages, but the actual adsorption site preference is not known. A theoretical attempt to determine the adsorption site preference by cluster calculations of a single adsorbed alkali-metal atom on the Cu(111) surface by Padilla-Campos *et al.*<sup>12</sup> was not able to give a clear answer. Their density-functional theory (DFT) calculation favored the on-top site while their Hartree-Fock calculation favored the hollow site for Na on Cu(111) indicating that Na, which lies between Li and K in the alkali-

metal series, has a less pronounced site preference.

The adsorption of alkali-metal atoms on a metal surface induces a charge redistribution at the interface between the alkali-metal adlayer and the substrate. According to the Gurney model,<sup>13</sup> the redistribution at low coverages has the character of a charge transfer to the substrate that is so large that the alkali-metal atoms have been considered to be ionized. Jellium calculations by Ishida<sup>14</sup> for Na on Al(111), on the other hand, show that the adsorbate-induced charge is localized in the intermediate region between the substrate and the adsorbate layer, indicating a more covalent character of the adsorbate-substrate bond.

The charge transfer creates a surface dipole which significantly decreases the work function of the system down to a minimum of  $\Phi_{\text{min}}^{\text{Na/Cu(111)}} = 2.2 - 2.6$  eV in the coverage range  $\theta = 0.12 - 0.22$ .<sup>9-11,15</sup> For higher coverages the work function increases, and for the saturated monolayer the work function approaches  $\Phi^{\text{Na/Cu(111)}} = 2.77 - 2.8$  eV.<sup>9,16</sup> The work function of the saturated monolayer is close to the bulk value of Na  $\Phi_{\text{bulk}}^{\text{Na}} = 2.75$  eV.<sup>17</sup>

Referring to the free-standing ordered Na monolayer and the clean Cu(111) surface, the adsorbate-substrate interaction will influence the band structure of both systems as the alkali-metal layer is adsorbed. Photoemission experiments<sup>15,19</sup> reveal that as the Na coverage is increased, the Shockley surface state decreases in energy from its zero coverage value 0.4 eV below the Fermi level at the center of the Brillouin zone,  $\bar{\Gamma}$ . Above  $\theta \approx 0.11$ , the surface state has moved down below the band edge of the local band gap at the Cu(111) surface and is no longer visible in the photoemission experiments.<sup>15,19</sup>

Two-photon photoemission experiments<sup>15</sup> indicate that there are unoccupied Na-induced states in the local band gap at the Cu(111) surface, which also decrease in energy with Na coverage. At higher coverage the Na-induced state of lowest energy becomes visible in ordinary photoemission experiment<sup>19</sup> and crosses the Fermi level at  $\theta \approx 0.35$ . At saturated monolayer coverage this state has reached the value 0.1 eV below the Fermi level at the  $\bar{\Gamma}$  point. The  $\bar{\Gamma}$  point energy of this state is located within the local band gap of the Cu(111) surface, which indicates that it is localized to the Na monolayer. Therefore this Na-induced state has been called a quantum-well state.<sup>6,18</sup>

There have been several attempts to model the quantum-well state by a phase-shift model based on experimental parameter values.<sup>18-21</sup> The results of the calculations were that the main amplitude of the wave function of the quantum-well state was located in the adlayer and decayed exponentially into the copper substrate. Bullet<sup>22</sup> has calculated the density of states of a Cu(111) surface covered by sodium, but there are no *ab initio* calculations of the electron structure for Na on Cu(111) which could verify the existence of the quantum-well states from *first-principles*. There is, however, a recent DFT calculation for the similar system Na on the Al(001) surface by Stampfl *et al.*<sup>23</sup> where they achieve good agreement between the calculated band-structure and photoemission data.

We have performed *ab initio* density-functional calculations in the supercell framework using the massively parallelized version of the computer code DACAPO.<sup>24</sup> The super-

cell method imposed periodicity on the possible adsorbate geometries that could be modeled. Therefore, we restricted our study to two ordered adsorption configurations, the  $(2 \times 2)$  structure corresponding to a submonolayer coverage of  $\theta = 1/4$  and the  $(3/2 \times 3/2)$  structure which is the saturated monolayer coverage of  $\theta = 4/9$ . To our knowledge, there is no experimental evidence that substitutional intermixing of the sodium adatoms and the copper atoms in the substrate surface layer occurs as has been observed for the related system Na on Al(111).<sup>25,26</sup> Consequently, only the on-surface adsorption was considered while the substitution process was omitted.

The adsorption geometries of these two Na adsorbate structures were investigated by comparing the binding energy of the Na layer at different high-symmetry sites on the Cu(111) surface. The energetically most favorable configurations of the two adlayer structures, including substrate relaxation, were later used to investigate the adsorbate-induced charge density and the electron structure at the corresponding coverages. The band structure of Na on Cu(111) was compared with the band structure of the clean Cu(111) surface and free-standing Na layers to characterize the Na-induced quantum-well states observed in photoemission experiments.<sup>6,15,18,19</sup>

## II. CALCULATIONS

The total energy calculations in this work were based on the density-functional theory (DFT).<sup>27,28</sup> The wave functions were expanded in a plane-wave basis set and the effective potential of the ions was described by ultrasoft pseudopotentials.<sup>29</sup> The use of ultrasoft pseudopotentials enabled good convergence for copper, already at a plane-wave energy cutoff of 350 eV, which was used in all slab calculations. The non-spin polarized version of the generalized gradient approximation (PW-91 GGA) (Ref. 30) was employed for the exchange-correlation functional. For a discussion of the accuracy of different versions of GGA functionals for the determination of chemisorption energies, see Hammer *et al.*<sup>31</sup>

The adsorbate-substrate system Na on Cu(111) was modeled by means of supercells with six layers of fcc-(111)-stacked copper atoms. We used single-sided adsorption for the adsorption structure determination and double-sided adsorption for the band-structure calculations. The atom positions on both sides of the slab in the band-structure calculations were determined by the results from the adsorption structure calculation. The single-sided supercell included seven layers of vacuum while the double-sided cell contained six layers of vacuum. To prevent the dipole field from the adsorbate side from interacting with the clean Cu(111) surface through the vacuum region in the single-sided calculations, we used the dipole correction.<sup>32</sup> The dipole correction compensated for the difference in work function between the sodium-covered side and the clean Cu(111) side of the slab, which also gave a direct estimation of the decrease in work function due to the sodium adsorption.

We considered two hexagonal adsorbate monolayer structures, the  $(2 \times 2)$  structure corresponding to the coverage  $\theta = 1/4$  and the saturated monolayer  $(3/2 \times 3/2)$  structure equivalent to  $\theta = 4/9$  coverage. The supercell of the  $(2 \times 2)$

TABLE I. Convergence test of the number of layers and the  $k$ -point sampling in the  $z$  direction.  $\Delta\Phi$  is the work-function change and  $\mu$  is the dipole moment.  $E_b$  is the binding energy calculated for the Na atom in the fcc site at  $(2 \times 2)$ -adsorbate structure using a different number of substrate layers.

Layers	MP grid	$\Delta\Phi$ (eV)	$\mu$ ( $e\text{\AA}$ )	$E_b$ (eV)
4	$(6 \times 6 \times 1)$	-2.794	0.358	1.9275
4	$(6 \times 6 \times 2)$	-2.797	0.359	1.9275
6	$(6 \times 6 \times 1)$	-2.846	0.365	1.9317
6	$(6 \times 6 \times 2)$	-2.852	0.366	1.9317
8	$(6 \times 6 \times 1)$	-2.830	0.363	1.9447
8	$(6 \times 6 \times 2)$	-2.834	0.364	1.9278

structure consisted of four copper atoms in each layer and one sodium atom in the adsorbate layer. Four different high-symmetry adsorption sites were considered, namely fcc and hcp hollow site, and bridge and on-top site.

The  $(3/2 \times 3/2)$  structure is more complicated to realize, because there is no possibility to form a hexagonal adlayer structure with a nearest-neighbor spacing of  $3/2$  times the underlying structure using only one type of adatom site. If either a top or a bridge site is chosen for the first adsorbate atom, a hexagonal lattice with  $3/2$  times nearest-neighbor spacing is obtained by one top site surrounded by six bridge sites. Similarly, a hexagonal  $(3/2 \times 3/2)$  layer can be established by a hollow site surrounded by six distorted hollow sites. Consequently, the  $(3/2 \times 3/2)$  structures were modeled by a supercell consisting of nine copper atoms in each substrate layer, ordered in a hexagonal  $(3 \times 3)$  pattern, and four sodium atoms placed in either of the two adlayer configurations described above.

To minimize the numerical error, all reference calculations of the clean Cu(111) surface and the free-standing Na monolayer were performed in the same supercell as the corresponding adsorbate system, except for the isolated Na atom calculation, which was performed in a cubic cell with  $12 \text{ \AA}$  side length. To calculate the spin-polarization energy of the Na atom, the Na atom calculation was performed both with and without the spin-polarized version of GGA.

To estimate the precision of the calculations, the variation in binding energy for the Na atom adsorbed in the fcc site of the  $(2 \times 2)$  structure was calculated as a function of the number of substrate layers and  $k$ -point sampling in the  $z$  direction. The binding energy for single-sided adsorption shown in Table I has converged already for four substrate layers, but to be able to use the same supercell for double-sided band-structure calculations we chose six substrate layers. Table I also shows that the use of one or two  $k$  points in the  $z$  direction yielded the same binding energy with reasonable precision.

A finite temperature smearing was used to diminish the number of  $k$  points necessary for convergence.<sup>33</sup> A Fermi distribution broadening of  $k_B T = 0.1 \text{ eV}$  seemed to be the optimal choice, which gave a reasonable number of  $k$  points while the energy offset from the  $T = 0 \text{ K}$  ground state remained very small. The Brillouin zone of the  $(2 \times 2)$  supercell was sampled by a Monkhorst-Pack grid<sup>34</sup> of  $(6 \times 6 \times 1)$  while the Brillouin zone of the  $(3/2 \times 3/2)$  supercell was divided into a Monkhorst-Pack grid of  $(4 \times 4 \times 1)$ ,

which yielded a comparable  $k$ -point sampling for the two supercells.

In order to take surface reconstruction effects into account, the atomic positions of the adsorbate atoms and the two uppermost substrate layers were relaxed. The atomic positions were optimized by a preconditioned Broyden-Fletcher-Goldfarb-Shanno (BFGS) algorithm<sup>32</sup> which minimizes the total energy as a function of the positions of the released ions. The relaxation was performed in three steps. First the atoms in the clean Cu(111)-surface slab were relaxed in the direction perpendicular to the surface to optimize the interlayer distances to remove internal forces in the substrate. Then the adsorbate atoms were relaxed vertically above a rigid substrate. Finally, both the adsorbate atoms and the two uppermost substrate layers were relaxed by a full, three-dimensional relaxation until the average force on each atom was less than  $10^{-2} \text{ eV/\AA}$ .

To determine the most favorable adsorption site after relaxation, the Na atom binding energy to the Cu(111) surface  $E_b$  was calculated for each adsorption site.  $E_b$  was defined as

$$E_b = [(E^{\text{Cu}(111)} + N E_{\text{atom}}^{\text{Na}}) - E^{\text{Na/Cu}(111)}] / N, \quad (1)$$

where  $E^{\text{Cu}(111)}$ ,  $E_{\text{atom}}^{\text{Na}}$ , and  $E^{\text{Na/Cu}(111)}$  are the total energies of the clean Cu(111) slab, the free Na atom, and the Na on Cu(111) adsorption system slab, respectively.  $N$  is the number of adsorbed sodium atoms in the supercell.

The interaction between the Na adsorbate atoms and the copper substrate can be analyzed by dividing the adsorption process into two steps, forming the Na layer in vacuum and adsorbing the Na layer on the Cu(111) surface. The cohesive energy of forming a free-standing Na layer in vacuum  $E_{\text{free}}^{\text{Na}}$  was defined as

$$E_{\text{free}}^{\text{Na}} = [N E_{\text{atom}}^{\text{Na}} - E_{\text{ML}}^{\text{Na}}] / N, \quad (2)$$

where  $E_{\text{ML}}^{\text{Na}}$  is the total energy of the free-standing Na monolayer.  $N$  is the number of sodium atoms in the monolayer cell.

Analyzing the adsorbate-induced charge density gives an understanding of the bonding character and the surface dipole responsible for the change in work function on a microscopic level. The induced charge-density plots are constructed by taking the difference between the charge density of the Na/Cu(111) slab and the sum of the charge density of the clean Cu(111) slab and the free-standing Na monolayer corresponding to the adsorbed structure,

$$\Delta\rho(\mathbf{r}) = \{\rho(\mathbf{r})^{\text{Na/Cu}(111)} - [\rho(\mathbf{r})^{\text{Cu}(111)} + \rho(\mathbf{r})_{\text{ML}}^{\text{Na}}]\}. \quad (3)$$

In addition, the local density of states (LDOS)  $\rho_{\mathbf{k},\epsilon}(\mathbf{r})$  was used to monitor the spatial distribution of specific states in the Brillouin zone. The LDOS was obtained by extracting the ultrasoft wave function  $\phi_{\mathbf{k},\epsilon}(\mathbf{r})$  with the desired energy eigenvalue in the specified  $k$  point from the total wave function. The pseudopotential augmentation charge at each atom  $Q_{mn}^I$  was added to the ultrasoft wave function in order to retain the physical weight of the one-particle Kohn-Sham wave function. The ultrasoft expression for the local density of states<sup>29</sup> is defined as

$$\rho_{\mathbf{k},\epsilon}(\mathbf{r}) = |\phi_{\mathbf{k},\epsilon}(\mathbf{r})|^2 + \sum_{m,n,I} Q_{mn}^I \langle \phi_{\mathbf{k},\epsilon}(\mathbf{r}) | \beta_m^I \rangle \langle \beta_n^I | \phi_{\mathbf{k},\epsilon}(\mathbf{r}) \rangle. \quad (4)$$

Finally, the band structure of the system was determined by calculating the Kohn-Sham eigenvalues along the irreducible wedge  $\bar{\Gamma}-\bar{M}-\bar{K}-\bar{\Gamma}$  of the surface Brillouin zone. The band structure of the  $(2 \times 2)$  structure was calculated in 232  $k$  points, while the band structure of the  $(3/2 \times 3/2)$  structure was calculated in 116  $k$  points.

The difference in periodicity of the Na adsorbate structure and the underlying structure of the copper substrate was employed in the analysis of the band structure. The supercell was determined by the unit cell of the adsorbate structure, which was larger than the unit cell of the copper substrate. This means that the substrate bands were not conveniently represented in the first Brillouin zone of the supercell. The different length scales of the adsorbate and substrate structures gave a method to discriminate between the substrate bands, which ‘‘bounced’’ at the zone boundaries and the center of the Brillouin zone, and the adsorbate-induced bands, which were properly described in the Brillouin zone.

In addition to this analysis, we compared the band structure of Na on Cu(111) with band structure of the clean Cu(111) surface, which enabled the identification of a number of Na-induced bands for the adsorption system. To estimate the dispersion of these bands, the energy eigenvalues of the Na-induced bands along the high-symmetry directions  $\bar{K}-\bar{\Gamma}-\bar{M}$  in the Brillouin zone were extracted and fitted to a free-electron parabola,

$$\epsilon(k) = \epsilon_{\bar{\Gamma}} + \frac{\hbar^2 k^2}{2m^*}, \quad (5)$$

where  $m^*$  is the band mass of the electron. The value of the band mass was then compared to the band mass in the corresponding free-standing Na monolayer. The extracted Na-induced bands were finally compared to the inverse-photoemission data for the  $(2 \times 2)$  structure<sup>10</sup> and to photoemission data for the saturated monolayer.<sup>16,19</sup>

### III. RESULTS

This section is divided into three parts. The first part deals with the adsorption structure of the two structures. The most favorable adsorption structure of each coverage is used in the second part to investigate the adsorbate-induced changes in the electronic charge distribution at the interface between the adsorbate layer and the substrate. In the third part, the new features in the band structure of the adsorbate system are analyzed using the information from the band structure of the clean Cu(111) surface and the free-standing Na layer. The Na-induced bands are then compared to photoemission experiments.

#### A. Adsorption structure

The site preference for Na on Cu(111) is a delicate matter since the Cu(111) surface is very smooth. In order to investigate the adsorption structure, we performed a two-step calculation where the Na adatom positions were first optimized

TABLE II. Properties of the adsorption system Na on Cu(111).  $\Phi^{\text{Na/Cu(111)}}$  is the work function of the system,  $\Delta\Phi$  is the work-function change,  $\mu$  is the dipole moment per adsorbate atom, and  $E_b$  is the Na binding energy per atom for Na adsorbed on Cu(111). The upper part of the table refers to the Na  $(2 \times 2)$ -adsorbate structure and the lower part to the Na  $(3/2 \times 3/2)$ -adsorbate structure.

Adsorption site	$\Phi^{\text{Na/Cu(111)}}$ (eV)	$\Delta\Phi$ (eV)	$\mu$ ( $e\text{\AA}$ )	$E_b$ (eV)
$(2 \times 2)$				
fcc	1.94	-2.86	0.37	1.944
hcp	1.95	-2.86	0.37	1.944
Bridge	1.95	-2.86	0.37	1.939
Top	1.98	-2.82	0.36	1.897
$(3/2 \times 3/2)$				
Hollow centered	2.73	-2.06	0.15	1.836
Top/Bridge	2.75	-2.05	0.15	1.833

above a rigid substrate and then the two uppermost substrate layers were relaxed together with the adsorbate atoms. The Na adsorption above a rigid substrate gave a rough indication of the site preference. The general trend was that hollow sites were the most favorable sites for the Na adsorption in contrast to the alkali-metal atoms heavier than Na, which prefer top sites.<sup>1</sup>

The substrate relaxation enabled rearrangement of the surface atoms to more favorable positions. The general result of the full relaxation of the adsorbate system was that the substrate showed a small tendency for substrate rumpling. Substrate atoms below sodium atoms were repelled into the substrate while substrate atoms with no sodium atom in the vicinity moved outward. The displacement was more pronounced the less the number of nearest neighbors for the adsorbate atom. Hence, adsorption on the top site generated the largest rumpling effect, where the substrate atom just below the on-top adatom was pushed inward a distance  $d = 0.1 \text{ \AA}$ . The substrate rumpling obviously diminished the difference between the adsorption sites because the least favorable site gained the most energy by buckling the substrate.

For the  $(2 \times 2)$  structure, adsorption at the fcc and hcp sites gave very similar results and corresponded to the largest binding energy after full relaxation, as can be seen in Table II. The difference in binding energy between the hollow site and the bridge site was, however, only 5 meV, which was of the same magnitude as the precision of the calculation. The binding-energy difference is obviously not decisive, but we placed the Na atom in the fcc-hollow site for the electron structure investigation of the  $(2 \times 2)$  structure. The relaxed position of the  $(2 \times 2)$ -sodium layer in the fcc site is shown in Fig. 1(a) and the optimized coordinates of the adsorbate and surface atoms are given in Table III.

When the nearest-neighbor distance of the adsorbate atoms in the  $(2 \times 2)$ -Na adlayer was reduced to form the saturated Na monolayer, it seemed probable that the Na monolayer had a hollow-site-centered structure. On the other hand, the binding energy/adsorbate atom resulted from an average over the binding energies of adatoms in different sites and many of the atoms in the hollow-site-centered structure in Fig. 1(b) were slightly off the high-symmetry sites. A com-

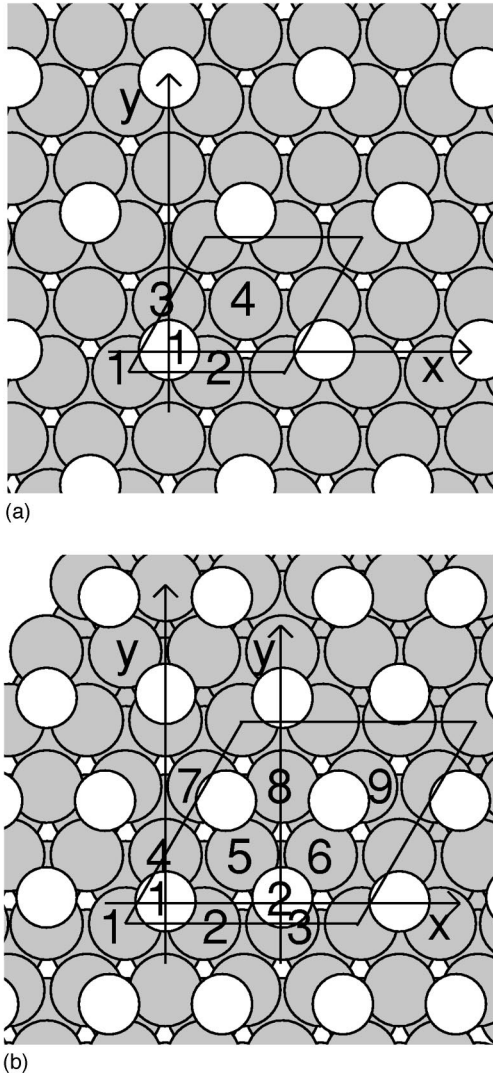


FIG. 1. The relaxed adsorption structure of the (a)  $(2 \times 2)$  structure and (b)  $(3/2 \times 3/2)$  structure. The supercell is indicated by a rhombus. The copper substrate atoms are gray and the sodium adatoms are white. The copper atoms are numbered from 1 to 4 for the  $(2 \times 2)$  structure and 1 to 9 for the  $(3/2 \times 3/2)$  structure. The sodium atom in the  $(2 \times 2)$  structure is numbered 1 and the two sodium atoms in the  $(3/2 \times 3/2)$  structure are numbered 1 and 2. The coordinates of the atoms in the supercell are shown in Table III.

parison of the values in Table II also reveals that the difference in binding energy/atom between the hollow-site-centered and the top/bridge adsorption structure was very small. The difference was as small as 3 meV/atom, which was below the precision of the calculations. In the end, the hollow-site-center adsorption structure was used for the electronic-structure calculation of the saturated monolayer. The final adsorption structure of the  $(3/2 \times 3/2)$  structure is shown in Fig. 1(b). The corresponding coordinates of the adsorbate and closest substrate atoms are given in Table III.

The slight preference for the hollow sites does not agree with the DFT results of the cluster calculations by Padilla-Campos *et al.*<sup>12</sup> However, our calculations are not directly comparable since they consider the low-coverage regime of isolated adsorbate atoms and we have studied higher coverages, where a significant adsorbate-adsorbate interaction is present.

TABLE III. The final adsorption structure after relaxation of the Na adsorbate atoms and the substrate. The coordinates are given with respect to the ideal center of mass of the three Cu atoms creating the hollow site before relaxation. The coordinate axes and the numbering of the atoms can be seen in Fig. 1.

Atom	$x$ (Å)	$y$ (Å)	$z$ (Å)
(a) fcc site, $(2 \times 2)$ structure			
Cu <sub>1</sub>	-1.31	-0.75	0.00
Cu <sub>2</sub>	1.30	-0.75	0.00
Cu <sub>3</sub>	-0.00	1.51	0.00
Cu <sub>4</sub>	2.59	1.49	0.08
Na <sub>1</sub>	-0.00	-0.00	2.40
(b) fcc site, $(3/2 \times 3/2)$ structure			
Cu <sub>1</sub>	-1.31	-0.76	0.04
Cu <sub>2</sub>	1.31	-0.76	0.04
Cu <sub>4</sub>	-0.00	1.51	0.04
Na <sub>1</sub>	-0.00	-0.00	2.51
(c) Distorted hollow site, $(3/2 \times 3/2)$ structure			
Cu <sub>3</sub>	0.00	-0.77	-0.10
Cu <sub>5</sub>	1.29	1.49	0.05
Cu <sub>6</sub>	1.30	1.49	0.05
Na <sub>2</sub>	0.00	0.08	2.47

To obtain a qualitative understanding of the relative importance of the adsorbate-adsorbate and the adsorbate-substrate interaction, we have divided the adsorption process into two steps. The Na layer was artificially formed in vacuum and in the next step placed on the substrate. The cohesive energy of the Na layer in vacuum is indicated as the dark gray regions in Fig. 2, while the light gray regions correspond to the energy gain when the Na layer is adsorbed on the Cu(111) surface.

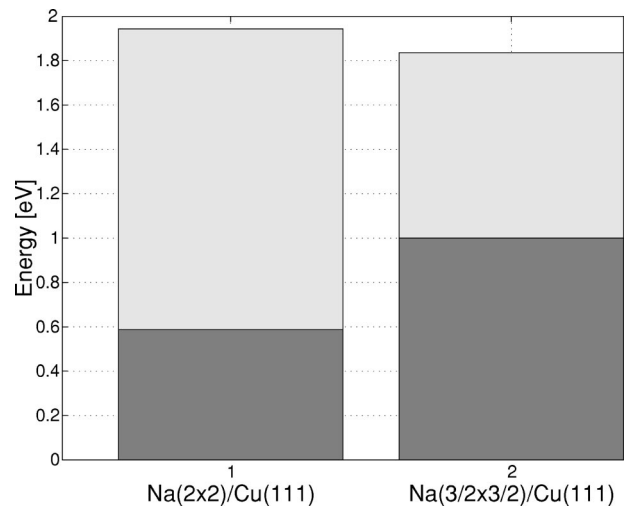


FIG. 2. The binding energy of Na on Cu(111) for the two adsorption geometries,  $\text{Na}(2 \times 2)/\text{Cu}(111)$  and  $\text{Na}(3/2 \times 3/2)/\text{Cu}(111)$ . The binding energy is divided into two contributions, the cohesive energy of forming a free-standing Na monolayer of corresponding structure (dark gray regions) and the energy gained by adsorbing the Na monolayer on the Cu(111) surface (light gray regions).

The cohesive energy of the free-standing hexagonal Na layer increases from  $E_{\text{free}}^{\text{Na}(2\times 2)} = 0.587$  eV for the  $(2\times 2)$  structure up to  $(3/2\times 3/2)$  value  $E_{\text{free}}^{\text{Na}(3/2\times 3/2)} = 1.00$  eV for the saturated monolayer indicating an attractive interaction between the atoms in the free-standing Na layer. To be able to compare the calculated value of the cohesive energy of the saturated monolayer to the spin-polarized all-electron calculation by Boettger and Trickey,<sup>35</sup> we have calculated the spin-polarization energy of the Na atom. We achieved a spin-polarization energy of  $-201$  meV, which lowers the cohesive energy to  $E_{\text{free}}^{\text{Na}(3/2\times 3/2)\text{Spin pol}} = 0.799$  eV in good agreement with the all-electron value of Boettger *et al.*,  $E_{\text{free}}^{\text{Na}(3/2\times 3/2)\text{AE}} = 0.81$  eV.

In contrast to the results for the free-standing Na monolayer, the binding energy of the adsorbed Na layer decreases with coverage, from  $E_b^{\text{Na}(2\times 2)/\text{Cu}} = 1.944$  eV to  $E_b^{\text{Na}(3/2\times 3/2)/\text{Cu}} = 1.844$  eV. This indicates an effective repulsive adsorbate-adsorbate interaction.

### B. Charge distribution

In the preceding subsection it was established that there was a slight preference for adsorption at hollow sites, but the difference in binding energy between the high-symmetry sites was very small. We will now turn to the character of the bonding between the adsorbate and the substrate.

The plots of the induced charge density in Fig. 3 and Fig. 4 reveal that upon adsorption of Na on Cu(111), the sodium charge is attracted toward the substrate. The charge redistribution creates a charge depletion in the Na layer and a charge accumulation at the interface between the Na layer and the Cu substrate. The charge accumulation is directed along the connecting lines between the Na adatoms and the nearest-neighbor atoms in the underlying Cu substrate. The redistribution maximum is localized between the adsorbate layer and the substrate. This charge redistribution indicates a metallic bond of covalent character.

The charge redistribution to form the adsorbate-substrate bond polarizes the adlayer. The polarization creates a surface dipole which is the main contribution to the notable decrease in work function from the value for the clean Cu(111) surface. Our calculated value of the work function of Cu(111) is  $\Phi^{\text{Cu}(111)} = 4.80$  eV, in agreement with the experimental value 4.85 eV by Gartland and Slagvold.<sup>36</sup> Tang *et al.*<sup>11</sup> monitored the coverage dependence of the work function and they obtained the minimum value  $\Phi_{\text{min}}^{\text{Na}/\text{Cu}(111)} = 2.4$  eV at  $\theta \approx 0.22$ . The calculated value of the work function for the  $(2\times 2)$  structure  $\Phi_{\text{DFT}}^{\text{Na}(2\times 2)/\text{Cu}(111)} = 1.94$  eV consequently underestimates the work function compared to the experimental value.

An increase of the coverage beyond the work-function minimum will increase the value of the work function until monolayer saturation occurs. The calculated value of the work function at the saturated monolayer  $\Phi_{\text{DFT}}^{\text{Na}(3/2\times 3/2)/\text{Cu}(111)} = 2.73$  eV is in agreement with the experimental value  $\Phi_{\text{Expt}}^{\text{Na}(3/2\times 3/2)/\text{Cu}(111)} = 2.8$  eV.<sup>11</sup>

Figure 4 shows that the charge redistribution for the saturated monolayer is considerable. There is a significant surface dipole also for the saturated monolayer which influences the work function of the system, as can be seen in Table II. Obviously the apparent agreement in the work function for

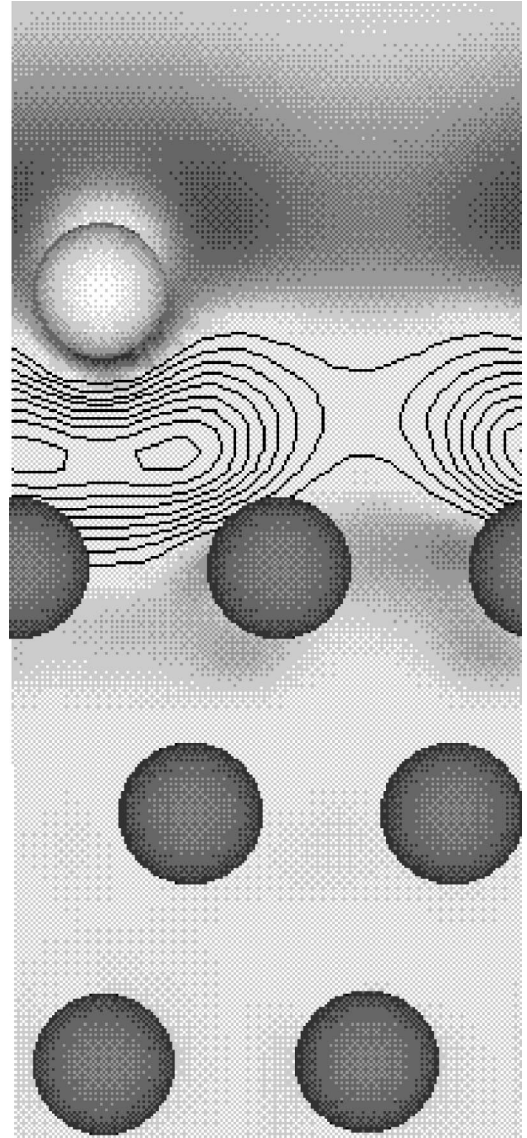


FIG. 3. The adsorbate-induced charge density  $\Delta\rho$  of the  $(2\times 2)$  structure. The Cu atoms are dark gray and the Na atoms are light gray. The charge accumulation is shown by isodensity lines of spacing  $2.5\times 10^{-3} e/\text{\AA}^3$  and the contour line of lowest value corresponds to  $2.5\times 10^{-3} e/\text{\AA}^3$ . The charge depletion is indicated by shading from black to white in the density range  $[-0.01, 0] e/\text{\AA}^3$ .

the Na/Cu(111) system at saturated monolayer coverage and the bulk material,  $\Phi^{\text{Na}} = 2.75$  eV,<sup>17</sup> is not an indication of a Na layer with bulk properties.

### C. Electron structure

The calculated adsorbate-induced charge density in Figs. 3 and 4 shows that the adsorption of Na on the Cu(111) surface leads to a charge redistribution at the interface. In this subsection, we analyze how this is reflected in the band structure and characterize the new states. We also compare our results to band structures extracted from photoemission experiments.<sup>10,15,19</sup>

The clean Cu(111) surface is the reference for the Na/Cu(111) system. Experimentally, the  $\bar{\Gamma}$  point energy of

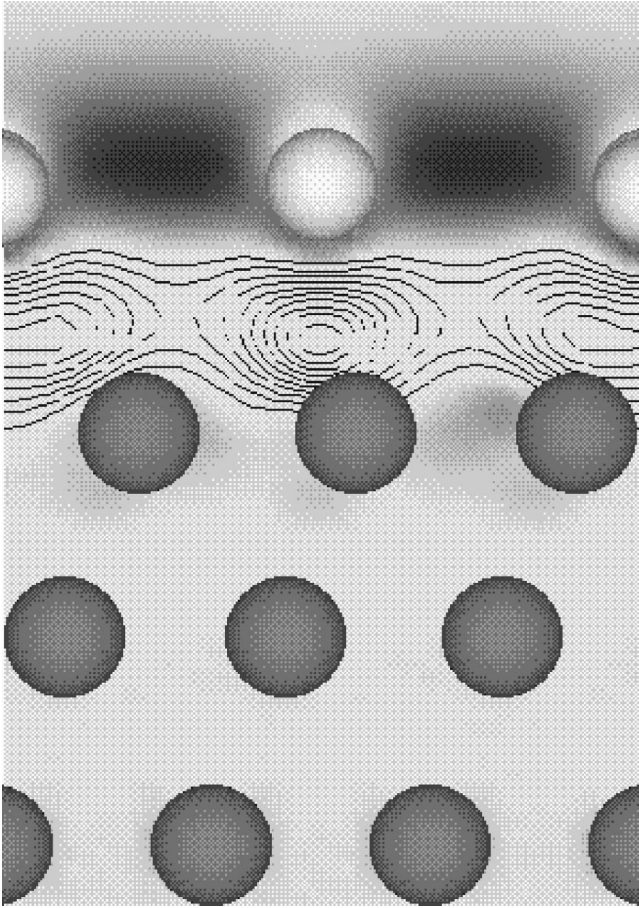


FIG. 4. The adsorbate-induced charge density  $\Delta\rho$  of the  $(3/2 \times 3/2)$  structure. The Cu atoms are dark gray and the Na atoms are light gray. The cut passes through the sodium adatoms. The charge accumulation is shown by isodensity lines of spacing  $2.5 \times 10^{-3} e/\text{\AA}^3$  and the contour line of lowest value corresponds to  $2.5 \times 10^{-3} e/\text{\AA}^3$ . The charge depletion is indicated by shading from black to white in the density range  $[-0.01, 0] e/\text{\AA}^3$ .

the Shockley surface state present at the Cu(111) surface is observed 0.4 eV below the Fermi level.<sup>36</sup> The calculated Shockley surface band was split into two bands in our reference calculation where a six-layer slab was used for the Cu(111) surface. The LDOS showed that there occurred an overlap between the surface states on opposite sides of the six-layer slab. This interaction between surface states on opposite sides of the slab caused the band splitting. We assumed that the band splitting was symmetric around the single band of an infinitely thick copper slab. The appropriate band could then be retrieved by taking the mean value of the band pair in each  $k$  point.

The calculated mean  $\bar{\Gamma}$  point energy of the Shockley surface state for the six-layer slab was then found 0.47 eV below the Fermi level. In an extended ten-layer slab calculation, the overlap decreased and the band splitting was less pronounced. In this case the surface state was found at 0.41 eV below the Fermi level in better agreement with experiment.

A comparison between the calculated band structure of the clean Cu(111) surface and the band structure of the  $(2 \times 2)$ -adsorbate structure in Fig. 5 reveals that two new pairs of unoccupied bands have emerged, indicated by thick solid

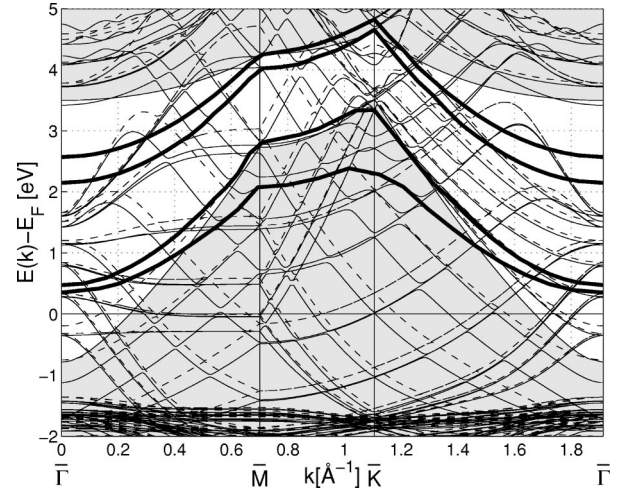


FIG. 5. The band structure of the Na $(2 \times 2)$ /Cu(111) structure (solid lines) and the corresponding band structure of the clean Cu(111) surface (dashed line). The shaded regions show the bulk copper bands projected onto the (111)-surface Brillouin zone. The copper bands appearing in the local band gap are folded bands, and the Na-induced bands are indicated by the thick solid lines.

lines. These are not present in the band structure of the clean surface. The splitting of these bands into pairs was due to interaction between the adsorbate layers on opposite sides of the slab, as for the surface state on the Cu(111) surface. This was confirmed by artificially displacing the Na  $(2 \times 2)$ -layer 1  $\text{\AA}$  away from the copper substrate, which reduced the band splitting. Checking the LDOS at the  $\bar{\Gamma}$  point for this state showed that there was an overlap between the states on opposite sides of the slab but the decay of the states was faster than for the Cu(111)-surface state which diminished the overlap. Therefore, we consider the energies of the Na-induced state to be more reliable than the energies of the copper surface state when six layers of copper are used as a copper substrate in the supercell.

We used the same mean value method to extract the appropriate band as described for the Cu(111)-surface state. The calculated bands with free-electron-like dispersion appeared in the local band gap of the Cu(111) surface. Furthermore, these bands apparently had the periodicity of the Na monolayer, indicating that they are Na-induced bands. To analyze the character of these bands, we compared their dispersion to the bands in free-standing Na layers in vacuum. We calculated the two-dimensional band structure for free-standing Na monolayers corresponding to both the  $(2 \times 2)$ - and the  $(3/2 \times 3/2)$ -adsorbate structure, as can be seen in Figs. 6 and 8. In comparison to earlier all-electron calculations by Wimmer<sup>37</sup> and Boettger and Trickey,<sup>35</sup> the agreement is satisfactory for the saturated Na monolayer.

To analyze the dispersion of the calculated bands along the  $\bar{K} - \bar{\Gamma} - \bar{M}$  line, the eigenvalues were fitted to the free-electron parabola in Eq. (5) by a least-square-fit method. The curve fits to the calculated bands are shown as the dashed lines in Figs. 6–9. The band masses are given in Table IV to enable a quantitative comparison. The bands of the free-standing Na monolayer and the Na-induced bands have a quasi-two-dimensional free-electron character and the corresponding band masses in Table IV are close, showing that

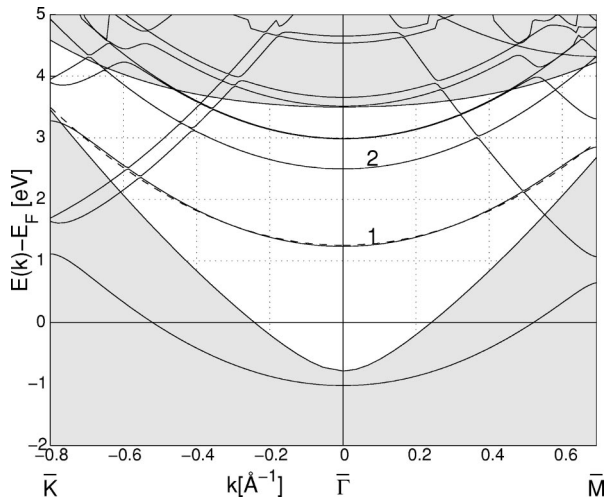


FIG. 6. The band structure of a free-standing Na monolayer in vacuum corresponding to the  $(2 \times 2)$ -adsorbate structure. The dashed lines indicate the parabolic fit to a free-electron parabola. The parameters can be found in Table IV. The bands used for comparison with the Na-induced bands are numbered 1 and 2. The shaded regions show the bulk copper bands projected onto the surface Brillouin zone with a Fermi level determined by the free-standing monolayer.

the Na-induced bands have a strong Na character and are not unduly affected by the adsorption to the substrate.

The two Na-induced bands in the local band gap for the  $(2 \times 2)$ -adsorbate structure can be interpreted as the unoccupied states that have been observed in the inverse-photoemission experiment by Dudde *et al.*<sup>10</sup> The authors characterize the lower state as a Na  $p_z$  state and the upper state as an image state pinned to the vacuum level. The dispersion of these states is mapped along the  $\bar{\Gamma} - \bar{M}$  and  $\bar{\Gamma} - \bar{K}$  directions in the Brillouin zone. In Fig. 7 the calculated Na-induced bands are compared to the experimental values,

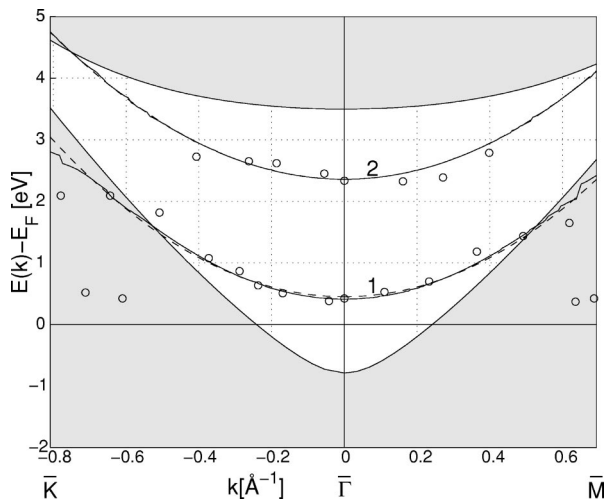


FIG. 7. The band structure of the Na $(2 \times 2)$ /Cu(111)-adsorbate structure. The solid lines are the Na-induced bands. The dashed lines show the curve fit to the free-electron parabola. The band index in Table IV is indicated by numbers. The shaded regions show the bulk band structure of copper projected onto the surface Brillouin zone. The circles are the inverse photoemission data from Dudde *et al.* (Ref. 10).

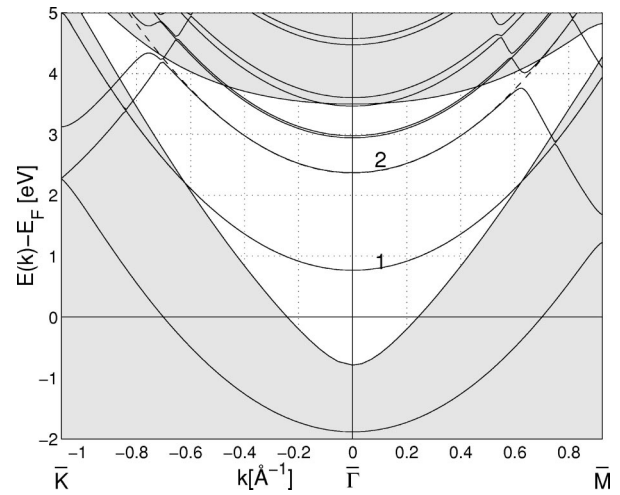


FIG. 8. The band structure of a free-standing Na monolayer in vacuum corresponding to the  $(3/2 \times 3/2)$ -adsorbate structure. The dashed lines indicate the parabolic fit of the energy eigenvalues to a free-electron parabola. The parameters can be found in Table IV. The bands used for comparison with the Na-induced bands are numbered 1 and 2. The shaded regions show the bulk copper bands projected onto the surface Brillouin zone with a Fermi level determined by the free-standing monolayer.

showing an excellent agreement for the lower band, though the experimental values are scattered around the calculated band. The experimental data points of the upper band show a similar spread around the calculated band, giving a qualitative agreement. On the other hand, the downshift of the work function for the  $(2 \times 2)$  structure is exaggerated in comparison with experiment,<sup>11</sup> which makes the upper calculated band less reliable. Consequently, the calculated values of  $m^*$  and the  $\bar{\Gamma}$ -point energy for the  $(2 \times 2)$ -adsorbate structure in

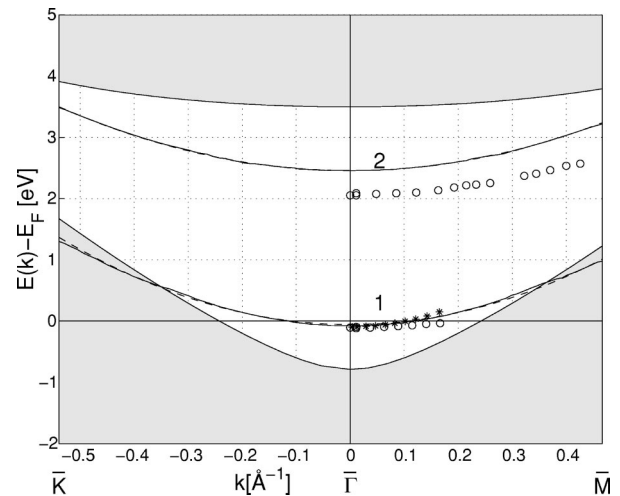


FIG. 9. The band structure of the Na $(3/2 \times 3/2)$ /Cu(111)-adsorbate structure. The solid lines are the Na-induced bands. The dashed lines show the curve fit to the free-electron parabola. The band index in Table IV is indicated by numbers. The shaded regions show the band structure of bulk copper projected onto the surface Brillouin zone. The LDOS of the lower band at the  $\bar{\Gamma}$  point is shown in Fig. 10. The circles and stars indicate the photoemission data from Fischer *et al.* (Ref. 16) and Carlsson *et al.* (Ref. 19), respectively.

TABLE IV. The calculated values of the  $\bar{\Gamma}$ -point energy  $\epsilon_{\text{DFT}}^{\bar{\Gamma}}$  relative to the Fermi level and the band mass  $m^*$ , of the Na-induced bands, obtained in the least-square fit to a free-electron dispersion parabola in Eq. (5). The values are given for the Na/Cu(111),  $(2 \times 2)$ , and  $(3/2 \times 3/2)$ -adsorbate structures (Fig. 7 and Fig. 9) and the corresponding free-standing Na monolayers in vacuum (Fig. 6 and Fig. 8). The band indexes are given in the figures. The calculated values are compared with the experimental values from Dudge *et al.*<sup>10</sup> for the  $(2 \times 2)$  structure, and Fischer *et al.*<sup>16</sup> and (Carlsson *et al.*<sup>19</sup>) for the  $(3/2 \times 3/2)$  structure.

Coverage system	$\epsilon_{\text{DFT}}^{\bar{\Gamma}}$ (eV)	$\frac{m_{\text{DFT}}^*}{m_e}$	$\epsilon_{\text{Exp}}^{\bar{\Gamma}}$ (eV)	$\frac{m_{\text{Exp}}^*}{m_e}$
Na( $2 \times 2$ ) band 1	1.26	1.09		
Na( $2 \times 2$ ) band 2	2.50	1.00		
Na( $2 \times 2$ )/Cu(111) band 1	0.45	0.96	0.56	1.22
Na( $2 \times 2$ )/Cu(111) band 2	2.36	1.04	2.39	1.70
Na( $\frac{3}{2} \times \frac{3}{2}$ ) band 1	0.80	1.06		
Na( $\frac{3}{2} \times \frac{3}{2}$ ) band 2	2.37	1.00		
Na( $\frac{3}{2} \times \frac{3}{2}$ )/Cu(111) band 1	-0.06	0.78	-0.11	1.4
			(-0.10)	(0.5)
Na( $\frac{3}{2} \times \frac{3}{2}$ )/Cu(111) band 2	2.46	1.06	2.07	1.3

Table IV are in agreement with the experimental values for the lower band, but there is a large difference in band mass for the image state.

Experiments<sup>15,19</sup> indicate that the  $\bar{\Gamma}$  point energy of the Na-induced states is coverage-dependent. The state of lowest energy shifts downward in energy as the coverage increases and the state becomes occupied at  $\theta \approx 0.35$ . At saturated monolayer coverage the measured energy of the state is  $\epsilon_{\text{Expt}}^{\text{Na}(3/2 \times 3/2)/\text{Cu}(111)} = -0.1$  eV with respect to the Fermi level.<sup>16,19</sup> The two experiments yield the same  $\bar{\Gamma}$  point energy, but they have significantly different dispersion in terms of the band mass for the occupied band, as can be observed in Fig. 9.

The calculated band structure for the  $(3/2 \times 3/2)$  structure showed two similar pairs of Na-induced bands as for the  $(2 \times 2)$  structure. One band pair was located around the Fermi level at the  $\bar{\Gamma}$  point and one pair was unoccupied. We performed a similar analysis of the dispersion of the Na-induced bands for the saturated Na monolayer as for the  $(2 \times 2)$  structure. The values of  $m^*$  in Table IV for the  $(3/2 \times 3/2)$ -adsorbate structure were close to the free-standing Na monolayer, indicating that the Na-induced bands had maintained the Na character also for the saturated monolayer. The calculated  $\bar{\Gamma}$  point energy of the occupied band was 0.06 eV below the Fermi level, in fair agreement with the experiments.<sup>16,19</sup> The dispersion in Fig. 9 is intermediate between the two experimental curves, which is satisfactory. The calculated unoccupied band has a slightly stronger dispersion than the two-photon photoemission<sup>16</sup> data and the  $\bar{\Gamma}$  point energy is shifted 0.4 eV above the experimental  $\bar{\Gamma}$  point value.

It is evident that the occupied part of the Na-induced band of lowest energy for the  $(3/2 \times 3/2)$  structure in Fig. 9 is

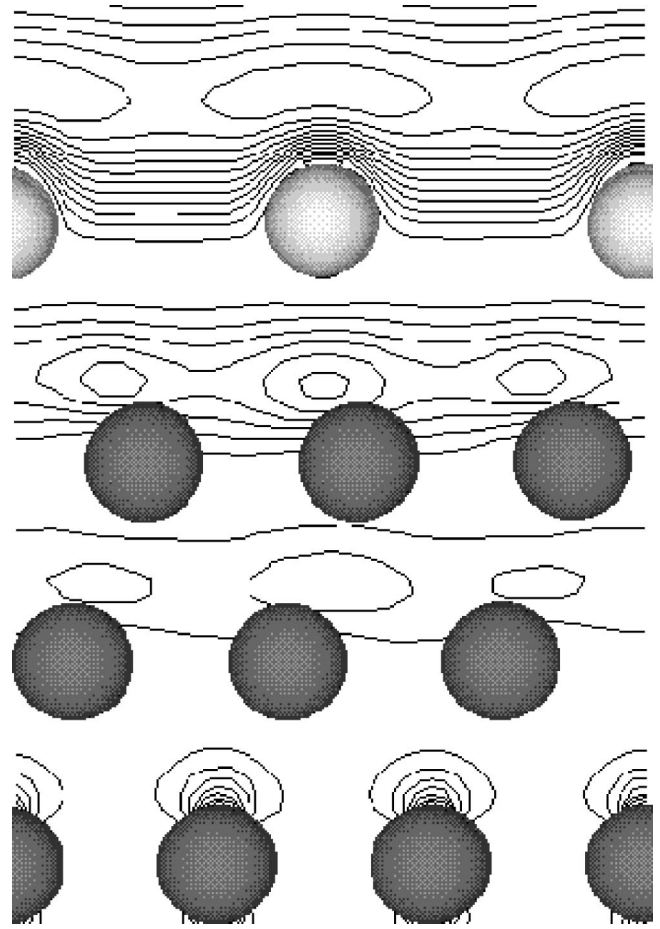


FIG. 10. The local density of states  $\rho_{\mathbf{k},\epsilon}(\mathbf{r})$  of the quantum-well state at the  $\bar{\Gamma}$  point for the saturated monolayer. The Cu atoms are dark gray and the Na atoms are light gray. The isodensity lines have a line spacing of  $5 \times 10^{-5} e/\text{\AA}^3$  and the contour line of lowest value corresponds to  $5 \times 10^{-5} e/\text{\AA}^3$ . The peak amplitude of this state is localized at the boundary between the Na layer and the vacuum boundary and the amplitude decays rapidly into the Cu substrate.

located within the local band gap of the Cu(111) surface near the  $\bar{\Gamma}$  point. This implies that the wave function of this state is localized in the adlayer and decays fast in the copper bulk. Monitoring the LDOS at the  $\bar{\Gamma}$  point in Fig. 10 reveals a maximum located in the interfacial region between the Na monolayer and the vacuum barrier. Another smaller maximum is located at the interface between the adlayer and the substrate and the amplitude decays rapidly as the wave function enters the substrate region, as expected. The distribution of the LDOS in real space of this state at the  $\bar{\Gamma}$  point agrees well with previous model calculations,<sup>18,20,21</sup> which supports the conclusion from these calculations. This Na-induced state has the quasilocalized character of a two-dimensional quantum-well state.

#### IV. SUMMARY

We have investigated an alkali-metal adsorption system, a monolayer of Na on Cu(111), in order to characterize its electron structure. Our aim was to study the possibility of forming quantum-well states in this system as suggested by

photoemission measurements. The analysis of the Na-induced electron structure is based on *first-principles* calculations of free-standing Na layers in vacuum, the clean Cu(111) surface, and the adsorbate system Na on Cu(111), for two different adsorption structures.

The adsorption of Na on the Cu(111) surface polarizes the system, giving rise to a large decrease of the work function. The polarization is due to a metallic bond of covalent character between the adsorbate layer and the copper substrate characterized by depletion of electron charge in the Na layer and a charge accumulation in the interface region.

The Na atoms have a slight preference for adsorption in hollow sites. However, the differences in the binding energy between different sites is in general a few meV, which indicates that the Cu(111) surface appears very smooth to the Na adsorbate atoms.

We have calculated the band structure of the adsorption system and analyzed the Na-induced bands. These bands are mainly located in the local band gap of the Cu(111) surface and the lower band is partly occupied at saturated monolayer coverage. The dispersion of the bands is essentially the same as the corresponding bands for free-standing Na layers.

Although we cannot expect to reproduce the unoccupied band structure in our DFT calculations, the agreement with experiments for most of the bands is good. We have in some details characterized the partly occupied and nearly parabolic Na band present at a saturated Na layer. The minimum of

this band is below the Fermi level at the  $\bar{\Gamma}$  point and well within the local band gap. Consequently, we expect the wave function at the  $\bar{\Gamma}$  point to be essentially confined to the adlayer region. The calculated local density of states reveals a large maximum at the adlayer/vacuum boundary, a smaller maximum at the interface between the adlayer and the copper substrate, and a fast decay into the substrate. We thus conclude that this state has the characteristics of a quantum-well state. Furthermore, the calculated  $\bar{\Gamma}$  point energy of the lowest Na-induced band for the two coverages is in agreement with the coverage dependence observed in photoemission experiments.

Our analysis suggests that the Na-induced band is a quantum-well band corresponding to states localized in the Na adlayer.

#### ACKNOWLEDGMENTS

This work has been supported by the Swedish Natural Science Research Council. The authors are in great debt to B. Hammer, L. Hansen, and L. Bengtsson for development and support of the DFT-code, DACAPO. The authors would also like to acknowledge L. Walldén, S.-Å. Lindgren, Y. Yourdshahyan, S. Mankefors, and C. Räsänen for stimulating discussions and suggestions on improving the manuscript.

- <sup>1</sup>R. Diehl and R. McGrath, Surf. Sci. Rep. **23**, 43 (1996).
- <sup>2</sup>C. Stampfl and M. Scheffler, Surf. Rev. Lett. **2**, 317 (1995).
- <sup>3</sup>J. J. Mortensen, B. Hammer, and J. K. Nørskov, Phys. Rev. Lett. **80**, 4333 (1998).
- <sup>4</sup>P. Sjövall, B. Hellsing, K.-E. Keck, and B. Kasemo, J. Vac. Sci. Technol. A **5**, 1065 (1987).
- <sup>5</sup>S.-Å. Lindgren and L. Walldén, Solid State Commun. **34**, 671 (1980).
- <sup>6</sup>S.-Å. Lindgren and L. Walldén, Phys. Rev. Lett. **59**, 3003 (1987).
- <sup>7</sup>D. Adler, I. Collins, X. Liang, S. Murray, G. Leatherman, K. Tsuei, E. Chaban, S. Chandravarkar, R. McGrath, R. Diehl, and P. Citrin, Phys. Rev. B **48**, 17 445 (1993).
- <sup>8</sup>A. Carlsson, D. Claesson, G. Katrich, S.-Å. Lindgren, and L. Walldén, Surf. Rev. Lett. **4**, 1233 (1997).
- <sup>9</sup>S.-Å. Lindgren and L. Walldén, Phys. Rev. B **22**, 5967 (1980).
- <sup>10</sup>R. Dudde, L. Johansson, and B. Reihl, Phys. Rev. B **44**, 1198 (1991).
- <sup>11</sup>D. Tang, D. McIlroy, X. Shi, and D. Heskett, Surf. Sci. Lett. **255**, L497 (1991).
- <sup>12</sup>L. Padilla-Campos, A. Toro-Labbe, and J. Maruani, Surf. Sci. **385**, 24 (1997).
- <sup>13</sup>R. W. Gurney, Phys. Rev. **47**, 479 (1935).
- <sup>14</sup>H. Ishida, Phys. Rev. B **42**, 10 899 (1990).
- <sup>15</sup>N. Fischer, S. Schuppler, Th. Fauster, and W. Steinmann, Surf. Sci. **314**, 89 (1994).
- <sup>16</sup>N. Fischer, S. Schuppler, Th. Fauster, and W. Steinmann, Phys. Rev. B **43**, 14 722 (1991).
- <sup>17</sup>H. B. Michaelson, J. Appl. Phys. **48**, 4729 (1977).
- <sup>18</sup>A. Carlsson, B. Hellsing, S.-Å. Lindgren, and L. Walldén, Phys. Rev. B **56**, 1593 (1997).
- <sup>19</sup>S.-Å. Lindgren and L. Walldén, Phys. Rev. B **38**, 3060 (1988).
- <sup>20</sup>B. Hellsing B., J. M. Carlsson, L. Walldén, and S.-Å. Lindgren, Phys. Rev. B **61**, 2343 (2000).
- <sup>21</sup>J. D. McNeill and C. B. Harris, Solid State Commun. **87**, 1089 (1993).
- <sup>22</sup>D. Bullet, Solid State Commun. **38**, 291 (1981).
- <sup>23</sup>C. Stampfl, K. Kambe, R. Fasel, P. Aebi, and M. Scheffler, Phys. Rev. B **57**, 15 251 (1998).
- <sup>24</sup>L. Hansen *et al.*, computer code DACAPO-1.30, CAMP, DTU, Denmark.
- <sup>25</sup>A. Schmalz, S. Aminpirooz, L. Becker, J. Haase, J. Neugebauer, M. Scheffler, D. R. Batchelor, D. L. Adams, and E. Bøgh, Phys. Rev. Lett. **67**, 2163 (1991).
- <sup>26</sup>J. Burchhardt, M. M. Nielsen, D. L. Adams, E. Lundgren, J. N. Andersen, C. Stampfl, M. Scheffler, A. Schmalz, S. Aminpirooz, and J. Haase, Phys. Rev. Lett. **74**, 1617 (1995).
- <sup>27</sup>P. Hohenberg and W. Kohn, Phys. Rev. **136**, B864 (1964).
- <sup>28</sup>W. Kohn and L. Sham, Phys. Rev. **140**, A1133 (1965).
- <sup>29</sup>D. Vanderbilt, Phys. Rev. B **41**, 7892 (1990).
- <sup>30</sup>J. Perdew, J. Chevary, S. Vosko, K. Jackson, M. Pederson, D. Singh, and C. Fiolhais, Phys. Rev. B **46**, 6671 (1992).
- <sup>31</sup>B. Hammer, L. Hansen, and J. K. Nørskov, Phys. Rev. B **59**, 7413 (1999).
- <sup>32</sup>L. Bengtsson, Ph.D. thesis, Chalmers University of Technology, Gothenburg, Sweden (1999).
- <sup>33</sup>M. J. Gillan, J. Phys.: Condens. Matter **1**, 689 (1989).
- <sup>34</sup>H. Monkhorst and J. Pack, Phys. Rev. B **12**, 5188 (1976).
- <sup>35</sup>J. Boettger and S. Trickey, J. Phys.: Condens. Matter **1**, 4323 (1989).
- <sup>36</sup>P. O. Gartland and B. J. Slagsvold, Phys. Rev. B **12**, 4047 (1975).
- <sup>37</sup>E. Wimmer, J. Phys. F: Met. Phys. **13**, 2313 (1983).